

Structural studies on ethylene–tetrafluoroethylene copolymer: 2. Transition from crystal phase to mesophase

Tetsuya Tanigami,* Kazuo Yamaura and Shuji Matsuzawa

Department of Chemistry, Faculty of Textile Science and Technology, Shinshu University, Ueda-shi, Nagano-ken 386, Japan

and Masazumi Ishikawa,† Keishin Mizoguchi‡ and Keizo Miyasaka

Department of Textile and Polymeric Materials, Tokyo Institute of Technology, Ookayama, Meguro-ku, Tokyo 152, Japan

(Received 16 August 1985; revised 20 December 1985)

A thermo-reversible, first-order transition from an orthorhombic crystal lattice to a hexagonal lattice (mesophase) was found in ethylene–tetrafluoroethylene alternating copolymer by using X-ray diffraction. The transition was shown to be the order–disorder transition with a wide pretransitional temperature range, which was caused by rotational motion around the chain axis as often observed in planar zigzag polymers like polyethylene. A characteristic anisotropy of the thermal expansion coefficient of the crystal lattice was observed in the pretransitional range. By combining dilatometric data with the X-ray data on crystal expansion, the copolymer composition, the fraction of ordered orthorhombic region in the crystal phase and the crystallinity were obtained. Furthermore, the relaxations observed in a dynamic viscoelastic measurement were analysed by comparison with the crystal expansion.

(Keywords: ethylene–tetrafluoroethylene copolymer; order–disorder transition; mesophase; pretransitional range; thermal expansion; dilatometry)

INTRODUCTION

In a previous paper¹, we proposed for the crystal structure of ethylene–tetrafluoroethylene alternating copolymer (ETFE) an orthorhombic unit cell with the following parameters: $a = 8.57 \text{ \AA}$, $b = 11.20 \text{ \AA}$ and c (chain axis) = 5.04 \AA . The unit cell consists of four planar zigzag chains. Although the molecular packing in the ab plane was determined to be like that of polyethylene (PE) crystal, it is impossible in such copolymers to determine the unit structure in three dimensions owing to irregular alternating order of two monomer units in the chain.

The alternating disorder also gives rise to the disordering in molecular packing with respect to the lateral direction of the chain¹. Further, the degree of packing order is much affected by sample preparation: the order is a good deal higher in one of the samples (sample B), which was prepared by melt extrusion and subsequent cooling under extension, than in the other samples, which were bulk crystallized from the melt. Owing to the lower packing order, the molecular packing observed in the latter samples was considered to be pseudo-hexagonal.

One of the other characteristics of ETFE is stiffness of the chain, which is due to tight packing of fluorine and hydrogen atoms in the chain direction. This stiffness

results in a higher tensile strength of ETFE than those of PE and polytetrafluoroethylene (PTFE)², and an increase in the melting temperature of ETFE, higher than that of PE. Although PE approaches a hexagonal phase near the melting point³, the phase cannot appear at one atmosphere owing to its low melting point. In contrast, the hexagonal phase has been observed in ETFE in this work. In other words, the high melting point of ETFE introduces the appearance of the mesophase (hexagonal phase) between crystal phase and isotropic melt. Here, the melting point denotes the transition point from the mesophase to the isotropic melt. One of the aims in this work is to clarify the transition from crystal phase to mesophase, which is just observable in PE as the pretransitional phenomenon, by using ETFE. We regard ETFE copolymer as a modified PE in which original hydrogen atoms are partially substituted by fluorine atoms with some regularity, not only for an industrial purpose, but also for studying the structure and property of PE.

EXPERIMENTAL

Samples

The samples used here were the same as those described in the previous report¹. Sample A was a uniaxially drawn and annealed film from a commercial unoriented ETFE film (Aflex, a product of Asahi Glass Co. Ltd, Japan). Sample B was an extruded and annealed film which was crystallized by cooling under extension from molten ETFE pellets (Aflon COP, also a product of Asahi Glass Co.).

* To whom correspondence should be addressed

† Present address: Central Engineering Laboratories, Nissan Motor Co. Ltd, Natsushima, Yokosuka-shi 237, Japan

‡ Permanent address: Industrial Research Institute, Yatabe-cho, Tsukuba-gun, Ibaraki-ken 305, Japan

Measurements

X-ray diffraction intensity curves were observed at various temperatures by using a Rigakudenki diffractometer. Ni-filtered $\text{CuK}\alpha$ radiation was used throughout this work. The sample temperature was controlled within $\pm 2^\circ\text{C}$ by passing in nitrogen gas at constant temperature. In experiments below room temperature, nitrogen gas evaporated from the liquid was used.

Dynamic viscoelastic properties of the sample were measured as a function of temperature by using a Toyoseiki Rheograph. The frequency was 10 Hz and the heating rate was 3°C min^{-1} . Dilatometry was conducted at a heating rate of $0.5^\circ\text{C min}^{-1}$.

RESULTS

Thermal expansion along the chain axis

Figure 1 shows a change of the X-ray meridional intensity curve for sample B with temperature. The two broad peaks at lower 2θ angles did not show any significant change with temperature in intensity and peak position. On the other hand, the other two somewhat sharper peaks at larger 2θ angles showed decrease of intensity with increasing temperature. These facts correspond well with the observation of Wilson and Starkweather⁴, who have stated that at the lower angles the 001 and 002 meridional reflections are covered with layer-line streakings, whereas at the higher angles the true 003 and 004 meridional reflections appear without such obscuration. Thus we employed in this study the most intense reflection 004 to monitor the thermal expansion of the crystal.

Figure 2 shows changes in spacing and integrated intensity from the 004 reflection with temperature. These changes were reversible in the temperature cycling. The chains in the crystal phase begin to shrink at about -110°C and the shrinkage becomes more pronounced above 70°C . Similar shrinkage has been observed for polymer crystals with planar zigzag chains such as PE⁵, poly(vinyl alcohol)⁶, and nylon-6⁷. Such shrinkage can be

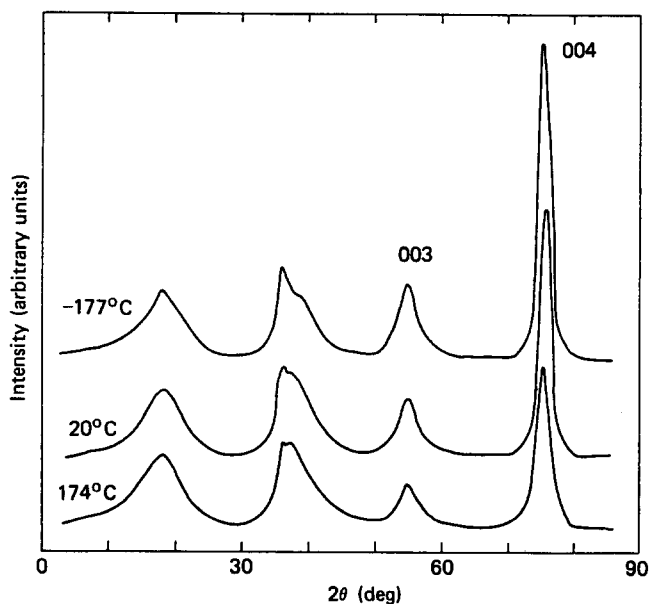


Figure 1 Meridional X-ray diffraction intensity curves of sample B at indicated temperatures

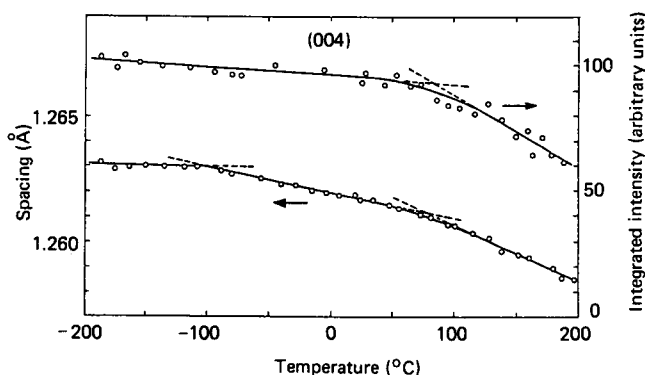


Figure 2 Variation of spacing and integrated intensity obtained from 004 meridional reflection with temperature

ascribed to torsional motion of the chains. The point of occurrence of the shrinkage will be related to γ -relaxation in dynamic viscoelastic properties. The remarkable shrinkage observed above 70°C associated with large decrease of intensity is related to the crystal transformation from the orthorhombic to the hexagonal lattice, as will be shown later. The thermal expansion coefficient of the c axis was $-8.2 \times 10^{-6} \text{ }^\circ\text{C}^{-1}$ between -100 and 80°C , and $-2.3 \times 10^{-5} \text{ }^\circ\text{C}^{-1}$ between 90 and 200°C . These values are comparable with those of PE crystal⁵: $-1.2 \times 10^{-5} \text{ }^\circ\text{C}^{-1}$ between 20 and 65°C and $-2.1 \times 10^{-5} \text{ }^\circ\text{C}^{-1}$ between 65 and 120°C . The shrinkage of ETFE is so small that the chain is considered to be planar zigzag throughout the temperature range of the measurements.

No distinction in the meridional intensity curve could be observed between samples A and B throughout the temperature range.

Thermal expansion in the ab plane

Sample B. Figure 3 shows X-ray equatorial intensity curves observed for sample B at various temperatures. The curves suggest a marked dimensional change induced thermally in the ab plane. The two peaks observed at low temperatures were indexed as 120 and 200 reflections in order of 2θ angle. The peaks became a single one at high temperature. The appearance of the intense single peak on the equator denotes a transition to hexagonal packing. The single peak was indexed as 100_h . From the change of the curve with temperature, the transition was considered to be reversible with temperature. Very weak equatorial reflections above $2\theta = 30^\circ$ gradually became less intense and very broad with increasing temperature. This indicates the decrease of long-range order.

The double peak of the 120 and 200 reflections was separated in the same way as reported in the previous paper¹. Thus calculated spacings from the reflections in Figure 3 are shown as a function of temperature in Figure 4. The unit-cell dimensions derived from the spacings in Figures 2 and 4 are shown in Figure 5, where the hexagonal lattice is regarded as an orthorhombic one, namely 'ortho-hexagonal' lattice. The a and b dimensions gradually approach one another through a wide temperature range from 0°C up to the transition point. We call the range and the point the 'pretransitional' range and T_h , respectively.

The integrated intensity and the halfwidth of the 120 and 200 reflections are shown in Figures 6 and 7, respectively. Below T_h the intensity ratio between the two

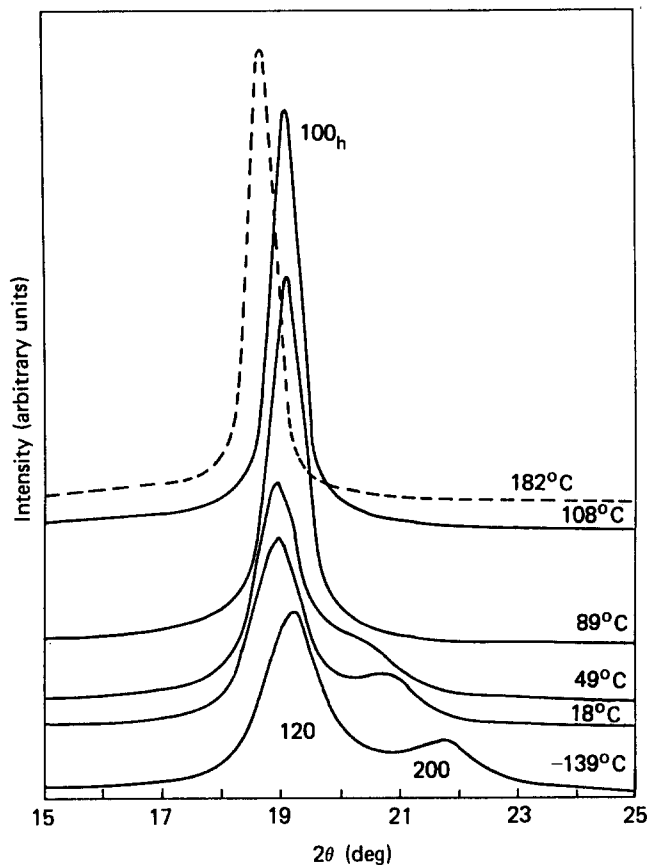


Figure 3 Equatorial X-ray diffraction intensity curves of sample B at various temperatures

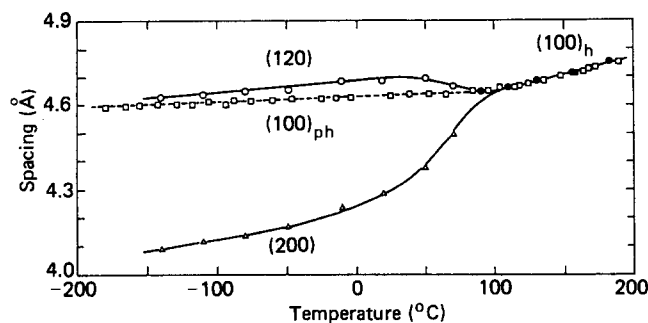


Figure 4 Variation of indicated spacings with temperature: —○— and —△—, (120) and (200) spacings of the orthorhombic lattice in sample B, respectively; —□—, (100)_{ph} spacing of the pseudo-hexagonal lattice in sample A; —■— and —●—, (100)_h spacings of the hexagonal lattices in samples A and B, respectively

reflections is almost constant. It indicates that the setting angle between the plane of the chain and the b axis, which is calculated from the ratio, did not change. On the other hand, the halfwidth decreased remarkably with temperature in the pretransitional range. This indicates the increase of one kind of short-range order, namely the packing order between the chains.

Sample A. As shown in Figure 8, the 120 and 200 reflections observed for sample A at room temperature apparently make a combined single but broad peak owing to the paracrystalline nature¹. The trailing of the peak to larger 2θ angles indicates the partial presence of ordered orthorhombic regions. Here, however, the lattice contained in sample A is regarded as a pseudo-hexagonal one which indexes the peak as 100_{ph} reflection. The same narrowing of the peak as in sample B was also observed as

shown in Figure 8. The spacing of $(100)_{ph}$ shows a slight change in the thermal expansion coefficient at T_h , as already shown by the broken line in Figure 4.

Figure 9 shows the integrated intensity and the halfwidth of the peak 100_{ph} as a function of temperature.

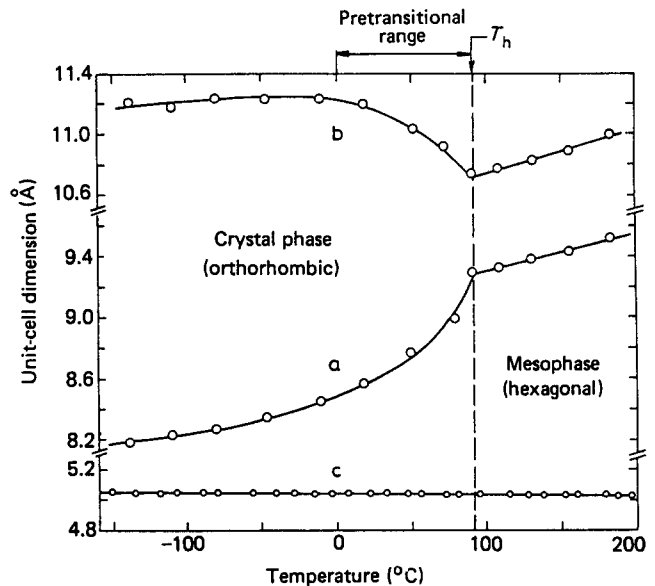


Figure 5 Variation of the unit-cell dimensions for the lattice observed in sample B with temperature

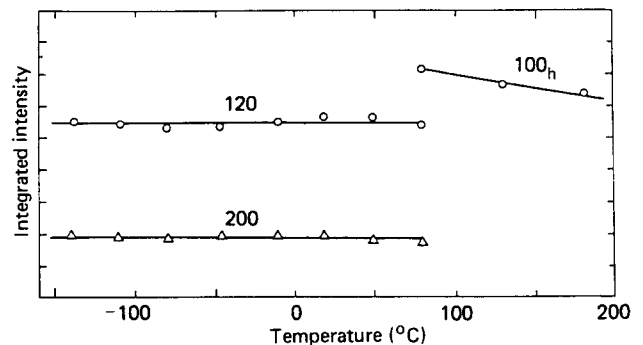


Figure 6 Variation of integrated intensity of the 120, 200 and 100_h reflections observed in sample B with temperature

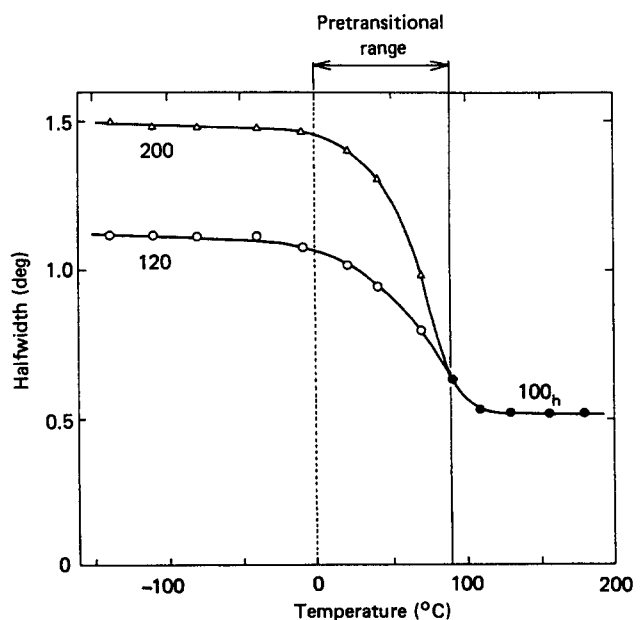


Figure 7 Variation of halfwidth of the reflection peaks observed in sample B with temperature

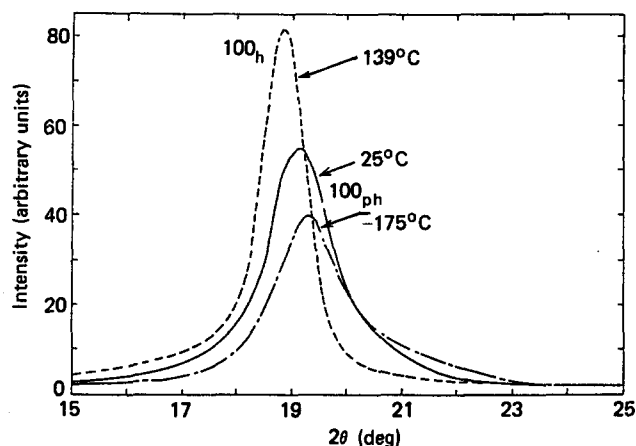


Figure 8 Equatorial X-ray diffraction intensity curves of sample A at various temperatures

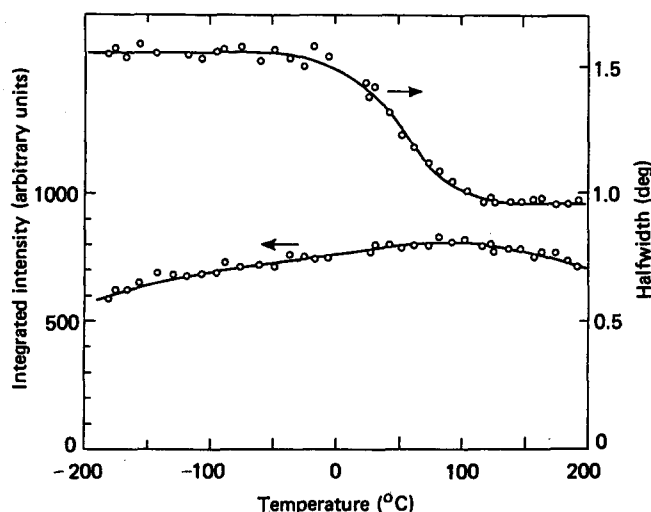


Figure 9 Variation of integrated intensity and halfwidth of 100_{ph} reflection peak observed in sample A with temperature

Two differences between samples A and B were found: one is a gradual increase of the integrated intensity with temperature up to T_h ; the other is that the halfwidth of 100_h is larger in sample A than in sample B. These may be related to the difference in the degree of the packing order. The order in sample A increased with increasing temperature, but it could not increase to the same level of order as in sample B even in the temperature range above T_h .

Thermal expansion of unit-cell volume

Figure 10 shows the thermal expansion of the unit-cell volume for samples A and B. The change of the volume at T_h indicates that the transition to the hexagonal lattice is clearly a first-order transition when from the orthorhombic lattice, while apparently a second-order transition when from the pseudo-hexagonal lattice. The volumetric thermal expansion coefficients are as follows: $2.8 \times 10^{-4} \text{ } ^\circ\text{C}^{-1}$ in the orthorhombic lattice, $4.9 \times 10^{-4} \text{ } ^\circ\text{C}^{-1}$ in the hexagonal lattice, and $7.0 \times 10^{-5} \text{ } ^\circ\text{C}^{-1}$ in the pseudo-hexagonal lattice. The first value is comparable to the value of $2.6 \times 10^{-4} \text{ } ^\circ\text{C}^{-1}$ for PE crystal between -196 and 130°C .⁸

It should be noted that the crystal phase of sample A consists of two regions; one is the ordered orthorhombic region and the other is the disordered pseudo-hexagonal one. Thus the actual unit-cell volume in the whole regions

of the crystal phase (V_c^A) would be an intermediate value between the pseudo-hexagonal (V_{ph}) and the orthorhombic (V_{or}) ones. Therefore, the change of the volumetric expansion coefficient at T_h for the whole crystal phase in sample A must be smaller than those for the pseudo-hexagonal region and the orthorhombic one.

Dynamic viscoelastic properties

Figure 11 shows the storage modulus E' , the loss modulus E'' and $\tan \delta$ for an unoriented sample A as functions of temperature. Four relaxations were observed: γ , β , α' and α in order of ascending temperature. The results shown are almost the same as those reported by Starkweather⁹ and Nishimura *et al.*¹⁰ The properties may be correlated with the crystal ones as follows: (1) chain shrinkage begins at the temperature where γ -relaxation was observed, as described above; (2) α' -relaxation is related to the pretransitional phenomenon of crystal transformation from the orthorhombic to the hexagonal lattices; and (3) the crystal transformation is completed at the temperature of α -relaxation at about 90°C , which has been assigned to the glass transition¹⁰.

Dilatometry

The specific volume of the crystal phase was estimated by using the dilatometric method of Price¹¹. Sample A was used for this measurement, because it was expected that the crystal phase in sample A could show a small and smooth change in volume at T_h as described above.

In Figure 12, open circles show the sample specific volume vs. temperature curve for sample A. The shape of the curve is the usual one as observed in crystalline polymers. Assuming that the volumetric change of the crystal phase at T_h was negligibly small compared with that in the amorphous phase at the glass transition point (T_g), T_g was determined to be 82°C as an intersection point (G) of the two straight lines A and B. The T_g value was almost the same as that from the $\tan \delta$ curve. The specific volume of the amorphous phase below T_m was drawn by an extrapolated line from that of the melt phase (line C) and line D which is parallel to line A and intersects with line C at T_g . The specific volume of the crystal phase, which contains both the pseudo-hexagonal region and the orthorhombic region, is expressed by line E which is parallel to line A and intersects with lines B and C at point R. The line E also expressed the specific volume of the hexagonal phase in its high-temperature region ($> T_h$).

The copolymer composition was derived by using the specific volume of the hexagonal phase ($v_h(T)$), which is shown by line E above T_h in Figure 12, and the unit-cell

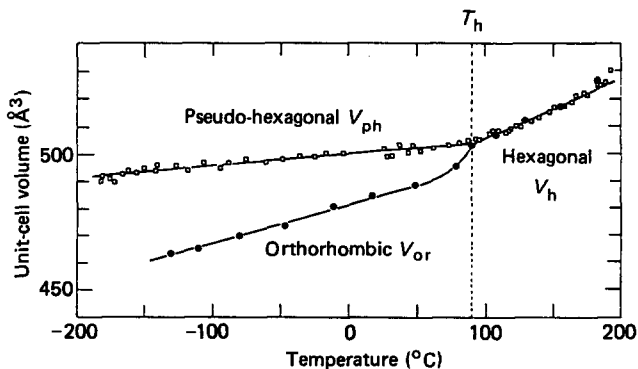


Figure 10 Volumetric thermal expansion of the unit cell for three phases indicated in the figure

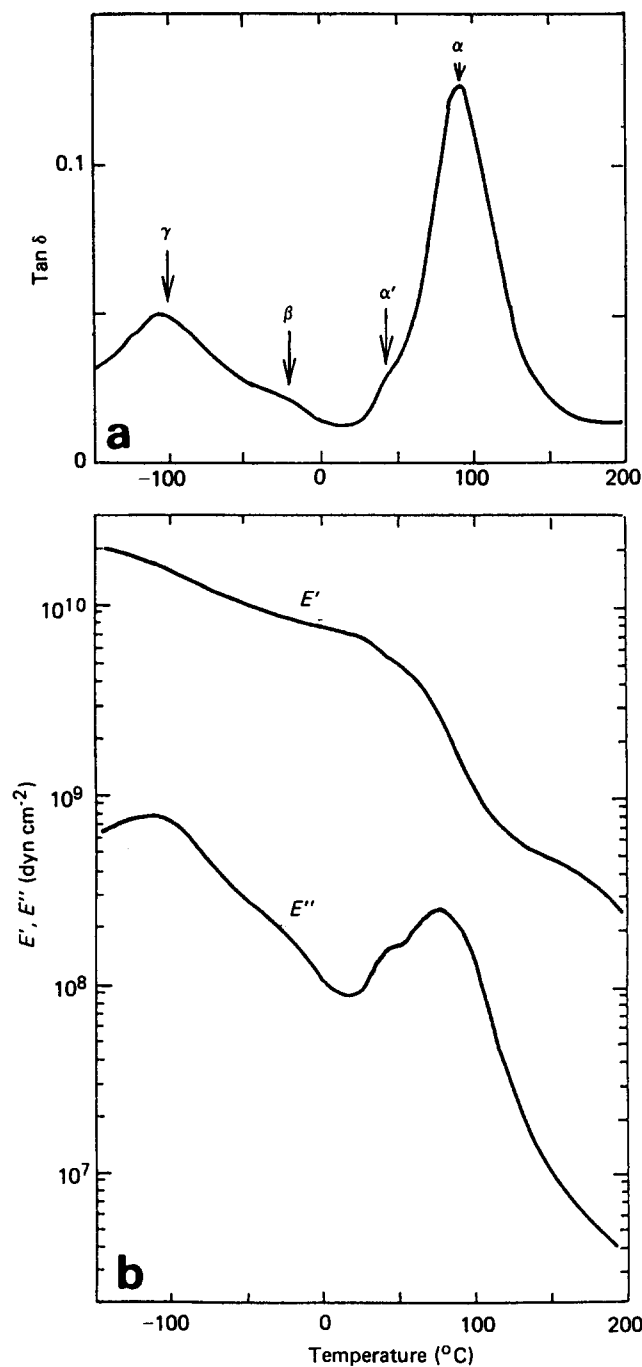


Figure 11 Dynamic viscoelastic properties for an unoriented sample A: (a) $\tan \delta$, and (b) E' and E'' as functions of temperature

volume of the hexagonal phase ($V_h(T)$) in Figure 10, as follows. First, the mole fraction of the ethylene unit (X_E) was assumed to be the same in the crystalline phase and the amorphous one. Then the molecular weight of the chemical repeating unit $(\text{CH}_2\text{CH}_2)_{2X_E}(\text{CF}_2\text{CF}_2)_{2(1-X_E)}$ was expressed by $M_w = 200 - 144X_E$. So v_h could be calculated by the following equation:

$$v_h(T) = V_h(T)N_A / (zM_w) \quad (1)$$

where z is the number of chemical repeating units in the unit cell (and here $z = 4$) and N_A is the Avogadro number. The parameter X_E was determined so that this $v_h(T)$ vs. temperature curve fitted with another $v_h(T)$ curve derived from the dilatometric measurement (line E in Figure 12) over the temperature range 90–170°C. The best fit was

achieved when $X_E = 0.473$, namely the copolymer composition was 47.3/52.7 mol%. Further, the chemical repeating unit was expressed as $(\text{CH}_2\text{CH}_2)_{0.946}(\text{CH}_2\text{CF}_2)_{1.054}$.

Once the composition was obtained, the specific volume of the orthorhombic crystal phase (v_{or}) and that of the pseudo-hexagonal one (v_{ph}) could also be calculated as a function of temperature by substituting the unit-cell volumes V_{or} and V_{ph} in Figure 10 respectively into equations analogous to equation (1), as shown in Figure 12. The total specific volume of crystal phase in sample A (v_c^A) had a value intermediate between v_{or} and v_{ph} . This indicates that the crystal phase in sample A has the ordered orthorhombic region and the disordered pseudo-hexagonal region. If the crystal phase is a mixture of the two regions, the weight fraction of orthorhombic region in crystal phase (x_{or}) can be estimated by using the following equation:

$$x_{or} = (v_{ph} - v_c) / (v_{ph} - v_{or}) \quad (2)$$

where the total specific volume of crystal phase (v_c) is regarded as v_c^A in sample A and v_{or} in sample B. The x_{or} is assumed to be 1.0 in sample B. Thus the estimated x_{or} value in sample A was 0.46 at 25°C and 0 at T_h . This means that the ordered region transforms into the disordered phase with increasing temperature.

The weight fraction of crystal phase (crystallinity) (X_c) was also estimated from the specific volume by the following equation:

$$X_c = (v_a - v_s) / (v_a - v_c) \quad (3)$$

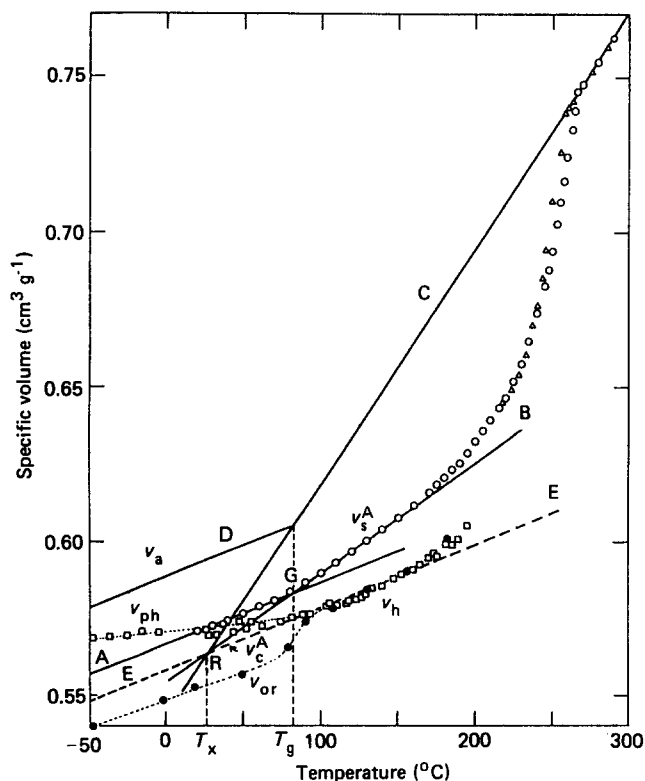


Figure 12 Specific volume of sample A (v_c^A) plotted against temperature. Open circles represent the specific volume vs. temperature curve in the heating process, and triangles that in the cooling process. The specific volumes of the other phases are also shown as functions of temperature: for the amorphous phase (v_a ; lines C and D), the crystal phase of sample A (v_c^A ; line E below T_h), the hexagonal phase (v_h), the pseudo-hexagonal crystal region observed in sample A (v_{ph}) and the orthorhombic crystal phase observed in sample B (v_{or}). The way of drawing these specific volumes is described in the text

where v_a is the specific volume of the amorphous phase, which was assumed to have the same value for all the samples and was estimated from line D. Here v_c denotes the total specific volume of the crystal phase, and v_s is the specific volume of the sample. The two weight fractions of x_{or} and X_c at 25°C for samples A and B are listed in Table 1, along with the specific volume (v) and the density (ρ). The density was calculated from the specific volume. It is noticeable that the density of the crystal phase in ETFE is variable with the degree of the packing order, which is controlled by sample preparation. The difference in crystal density ($\rho_c^A < \rho_c^B$) introduced the noteworthy fact that sample A with lower sample density than sample B showed higher crystallinity than sample B.

DISCUSSION

Order-disorder transition from crystal phase to mesophase

The transition from the orthorhombic phase to the hexagonal one is most skilfully characterized by the narrowing of the two reflections at low 2θ angles. The narrowing indicates an increase of the packing order of the chains with respect to their lateral direction. As reported on polymers with a transition to the hexagonal phase, such as PTFE¹²⁻¹⁴, a high-pressure phase of PE¹⁵⁻¹⁷, poly(*trans*-1,4-butadiene)¹⁸⁻²⁰ and some poly(organophosphazenes)^{21,22}, the ordering in the packing is considered to be caused by increased rotational motion of the chains around the chain axes. Although the rotational motion in this case increases only the short-range order of the packing order, it decreases the degree of both the other short-range order and the long-range order. Thus, the transition is said to be an order-disorder transition. In the hexagonal phase, the rotational motion should be so thoroughly activated in the whole chains in the crystal phase that the phase is regarded as a two-dimensional crystal and called mesophase. In the pretransitional range, the motion is activated locally in the crystal phase and the fraction of activated chains increases with temperature. This means the gradual approach to the hexagonal phase and apparently introduces the nature of a second-order transition into this first-order transition.

One remarkable feature of ETFE crystal is the disordered packing of the chains due to an avoidable alternating disorder of two monomer units¹. Further, the degree of the packing order depends on the sample preparation and cannot be changed by heating to the

mesophase and subsequent recooling to the crystal phase. Interestingly, the difference in the degree of packing order between samples A and B in the crystal phase lies in the mesophase.

Anisotropy of the thermal expansion of the lattice

The thermal expansion coefficient is a two-rank tensor. In the case of orthorhombic crystals, the principal axes of the tensor are consistent with those of the unit cell. The principal tensor for ETFE is given by

$$\begin{bmatrix} \alpha_a & 0 & 0 \\ 0 & \alpha_b & 0 \\ 0 & 0 & \alpha_c \end{bmatrix}$$

where the components α_a , α_b and α_c represent the thermal expansion coefficients in directions of the a , b and c axes, respectively. The coefficient in an optional direction in the ab plane can be expressed as a function of an azimuth angle (ω) made by the a axis and temperature (T):

$$\alpha(T, \omega) = \alpha_a(T) \cos^2 \omega + \alpha_b(T) \sin^2 \omega \quad (4)$$

We substituted the observed coefficients from Figure 5 into equation (4) to obtain anisotropic patterns of the coefficient shown in Figure 13. An isotropic expansion coefficient for the melt was obtained from the dilatometry in Figure 12. The shapes of the patterns are two-leaved, four-leaved, discoid and spherical in order of increasing temperature. The most remarkable pattern is the four-leaved one observed in the pretransitional range. It seems that the gradual but large increase in thermal expansion coefficient along the a axis continuously decreases the expansion coefficient along the b axis to a negative value. It is meaningful that the appearance of the four-leaved pattern is regarded as a pretransitional expansion for the order-disorder transition.

Comparison of the thermal expansion between ETFE and PE

In Figure 14 the changes of axis ratios a/b' for ETFE crystal and a/b for PE crystal with temperature are compared with one another. The full curve for PE is that observed by Swan³ and the broken curve for PE is that arbitrarily assumed above the melting temperature. As mentioned previously³, the same pretransitional expansion as that of ETFE appears slightly in PE just

Table 1 Specific volume ($\text{cm}^3 \text{g}^{-1}$) [density (g cm^{-3})], weight fraction of orthorhombic region in crystal phase and weight fraction of crystal phase (crystallinity) at 25°C

Sample	Sample, v_s [ρ_s]	Amorphous phase, v_a [ρ_a]	Crystal phase			Weight fraction of orthorhombic region in crystal phase, x_{or}	Weight fraction of crystal phase (crystallinity), X_c
			Orthorhombic region, v_{or} [ρ_{or}]	Pseudo-hexagonal region, v_{ph} [ρ_{ph}]	Total, v_c [ρ_c]		
Sample A	0.572 [1.749]	0.594 [1.684]	0.553 ^a [1.807]	0.571 [1.750]	0.563 [1.775]	0.46	0.72
Sample B	0.568 ^b [1.762]	0.594 ^c [1.684]	0.553 [1.807]	—	0.553 [1.807]	1.00	0.65

^a Assumed to be the same as crystal specific volume of sample B

^b Calculated from density measured in the previous work

^c Assumed to be the same as that of sample A

ETFE than of PE. Further, we expect that ETFE crystal would be a model crystal to investigate the other general features of polyethylene-type crystals.

CONCLUSION

The chain conformation can be regarded as a planar zigzag one throughout the temperature range of our measurements, although the chain shrinks slightly with increasing temperature with a similar negative thermal expansion coefficient to that of PE crystal.

The observed first-order transition from the orthorhombic phase to the hexagonal one is an order-disorder transition with a wide pretransitional range.

The motive force of the transition is considered to be rotational motion of the molecules around the chain axes.

The hexagonal phase is called the mesophase, since the phase has only two-dimensional order for rotational motion, which is the intermediate order between the crystal phase and the isotropic melt.

The appearance of four-leaved pattern in the anisotropy of thermal expansion coefficient of the crystal lattice can be regarded as a pretransitional phenomenon for the order-disorder transition.

A transition with the same mechanism as described above is observed apparently as a second-order transition from the pseudo-hexagonal lattice to the hexagonal one in sample A, since the crystal phase has partly paracrystalline disorder.

The analysis of the specific volume vs. temperature curve of sample A yields 47.3/52.7 mol% for the

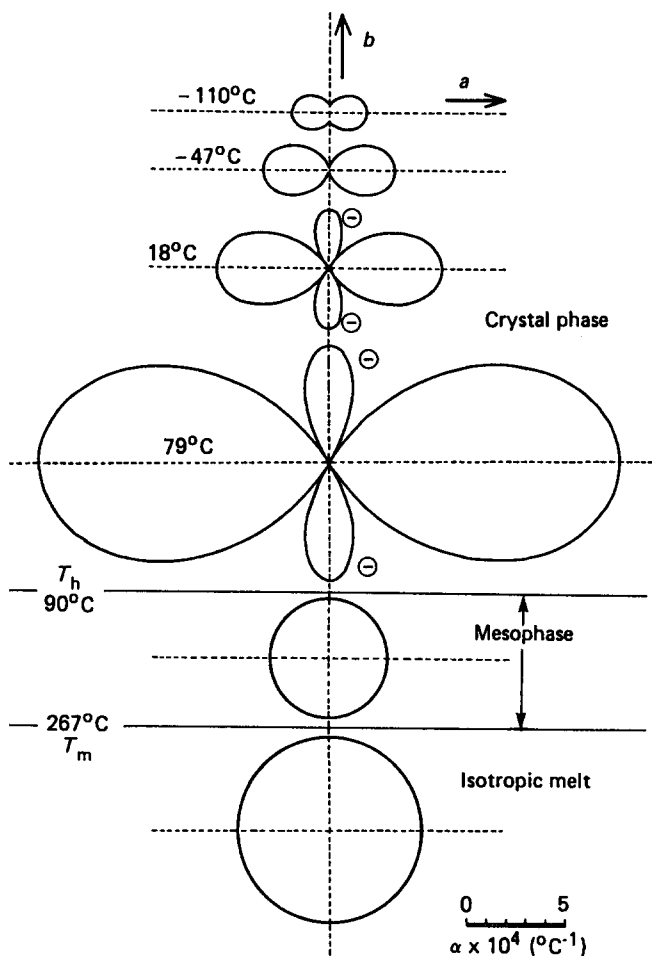


Figure 13 Anisotropic patterns of thermal expansion coefficient of orthorhombic crystal phase, mesophase and melt of ETFE are drawn in ab plane at indicated temperatures. The patterns for the former two phases are calculated from the X-ray diffraction data in Figure 5, and the pattern for the isotropic melt is from the dilatometric data in Figure 12

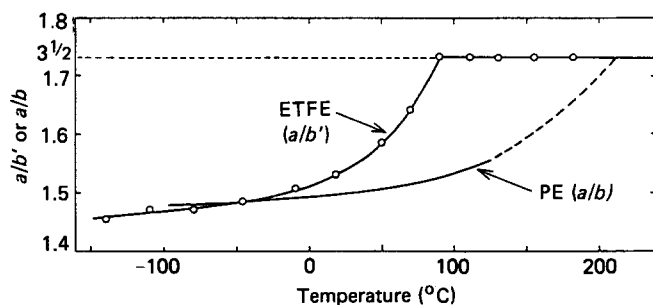


Figure 14 Comparison of the ratio of the unit-cell axes of ETFE (a/b') against PE (a/b). b' represents the subcell axis of the orthorhombic unit cell ($b' = b/2$) and see ref. 1 for details

below the melting point. This can be expressed more visually by the anisotropic pattern as shown in Figure 15. Here, however, the pretransitional range is so narrow that the negative expansion coefficient along the b axis cannot increase. Further, the mesophase does not appear in PE.

Hayakawa and Wada calculated lattice parameters for PE as a function of temperature by using the molecular field approximation²³. They successfully explained the increase of the a axis, decrease of the b axis and constancy of the setting angle with increasing temperature. It seems that these characteristics of the planar zigzag chains expected by them for the order-disorder transition could be ascertained more conspicuously by observation of

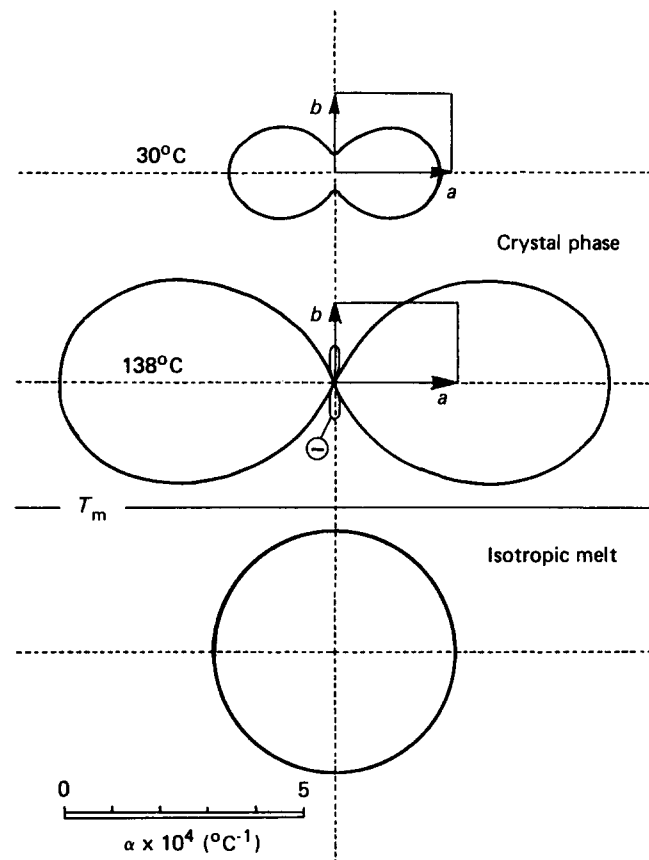


Figure 15 Anisotropic patterns of the thermal expansion coefficient of the orthorhombic crystal phase and the melt for PE are drawn in the ab plane at indicated temperatures. The pattern of the crystal phase is calculated from Swan's data³, and that of the isotropic melt is from the dilatometric data²⁴

copolymer composition of CH₂CH₂/CF₂CF₂ and 46% for the fraction of ordered orthorhombic crystal region at 25°C.

This fraction cannot be increased by recrystallization from the mesophase.

Tan δ vs. temperature curve for an unoriented sample A shows four relaxations: γ , β , α' and α . The shrinkage of the chain occurs with the γ -relaxation. The α' -relaxation is observed at an intermediate temperature of 50°C in the pretransitional range between 0 and 90°C. And the α -relaxation at about 90°C corresponds to the glass transition, which is also observed at 82°C by dilatometry.

ACKNOWLEDGEMENT

We thank Asahi Glass Co. Ltd for supplying us with the samples used in this study.

REFERENCES

- 1 Tanigami, T., Yamaura, K., Matsuzawa, S., Ishikawa, M., Mizoguchi, K. and Miyasaka, K. *Polymer* 1986, **27**, 999
- 2 Koyama, R. and Satokawa, T. *Yuki Gosei Kagaku Kyokaishi* 1973, **31**, 518
- 3 Swan, P. R. *J. Polym. Sci.* 1962, **56**, 403
- 4 Wilson, F. C. and Starkweather, H. W., Jr. *J. Polym. Sci., Polym. Phys. Edn.* 1973, **11**, 919
- 5 Kobayashi, Y. and Keller, A. *Polymer* 1970, **11**, 114
- 6 Shirakashi, K., Ishikawa, K. and Miyasaka, K. *Kobunshi Kagaku* 1964, **21**, 588
- 7 Miyasaka, K., Isomoto, T., Koganeya, H., Uehara, K., Ishikawa, K. and Ogata, N. *J. Polym. Sci., Polym. Phys. Edn.* 1980, **18**, 1047
- 8 Swan, P. R. *J. Polym. Sci.* 1960, **42**, 525
- 9 Starkweather, H. W., Jr. *J. Polym. Sci., Polym. Phys. Edn.* 1973, **11**, 587
- 10 Nishimura, H. and Yamabe, M. *Rep. Res. Lab. Asahi Glass Co. Ltd* 1974, **24**, 59
- 11 Price, F. P. *J. Chem. Phys.* 1951, **19**, 973
- 12 Clark, E. S. and Muus, L. T. *Z. Krist.* 1962, **117**, 108 and 119
- 13 Matsushige, K., Enoshita, R., Ide, T., Yamauchi, N., Taki, S. and Takemura, T. *Jpn. J. Appl. Phys.* 1977, **16**, 681
- 14 Yamamoto, T. and Hara, T. *Polymer* 1982, **23**, 521
- 15 Bassett, D. C. in 'Developments in Crystalline Polymers I', (Ed. D. C. Bassett), Applied Science Publishers, London, 1982, Ch. 3
- 16 Yasuniwa, M., Enoshita, R. and Takemura, T. *Jpn. J. Appl. Phys.* 1976, **15**, 1421
- 17 Yamamoto, T., Miyaji, H. and Asai, K. *Jpn. J. Appl. Phys.* 1977, **16**, 1891
- 18 Tatsumi, T., Fukushima, T., Imada, K. and Takayanagi, M. *J. Macromol. Sci.-Phys.* 1967, **B1**, 459
- 19 Iwayanagi, S. and Sakurada, I. *J. Polym. Sci.* 1966, **C15**, 29
- 20 Suehiro, K. and Takayanagi, M. *J. Macromol. Sci.-Phys.* 1970, **B4**, 39
- 21 Schneider, N. S., Desper, C. R. and Beres, J. J. in 'Liquid Crystalline Order in Polymers', (Ed. A. Blumstein), Academic Press, New York, 1978, Ch. 9
- 22 Matsuzawa, S., Yamaura, K., Tanigami, T. and Higuchi, M. *Colloid Polym. Sci.* 1985, **263**, 888
- 23 Hayakawa, R. and Wada, Y. *Rep. Prog. Polym. Phys. Jpn.* 1968, **11**, 215
- 24 Chiang, R. and Flory, P. J. *J. Am. Chem. Soc.* 1961, **83**, 2857